

Table of Contents

Cover pages and budget summary

Table of contents

Summary of proposal, personnel, and effort

Scientific/technical/management section (15 pages)

1 - Introduction

2 - SPICAM

3 - Previous Results from SPICAM ρ , p , T Profiles

4 - Task 1: Comparison of SPICAM Data, Accelerometer Data, and Model Predictions

5 - Task 2: Formation and Analysis of Composite T(p) Profiles From Surface to 200 km

6 - Task 3: Effects of Thermal Tides in SPICAM Data

6.1 - Summary: Thermal Tides

6.2 - Description of Task 3

7 - Task 4: Effects of Dust Storms on SPICAM Data

8 - Impact of Additional SPICAM Data and MCS Data

9 - Anticipated Results and Broader Implications

10- Relevance to NASA Programs

11 - Personnel

12 - Work Plan

References

Biographical Sketch for PI Paul Withers

Biographical Sketch for Co-I Jean-Loup Bertaux

Biographical Sketch for Co-I John Clarke

Current and Pending Support for PI Paul Withers

Current and Pending Support for Co-I Jean-Loup Bertaux

Current and Pending Support for Co-I John Clarke

Letter of Commitment from Co-I Jean-Loup Bertaux

Letter of Commitment from Co-I John Clarke

Letter of Commitment from Collaborator Franck Montmessin

Summary of Personnel and Effort

Budget Narrative

Facilities and Equipment

Title: Analysis of SPICAM stellar occultation data

Short title: Analysis of SPICAM stellar occultation data

Summary of proposal:

A Boston University-Service d'Aeronomie team will use SPICAM density, pressure, and temperature profiles to study the dynamics and thermal structure of the martian atmosphere between 50 km and 150 km. Task 1. SPICAM data, aerobraking accelerometer data, and theoretical predictions from Bougher's model will be compared to test this widely-used model. Task 2. TES, SPICAM, and MRO accelerometer data will be combined to form composite T(p) profiles from the surface to 200 km. These composite profiles will provide a top-to-bottom view of the atmosphere comparable only to the two Viking entry profiles. Task 3. Thermal tides are a major part of upper atmospheric dynamics and greatly affect aerobraking and accelerometer measurements. A different set of tides dominates lower atmospheric observations. SPICAM data will be used to study these tides in the middle atmosphere transition region. Task 4. A few observations have shown that dust storms affect the middle and upper atmosphere, but lack of observations has prevented detailed study. SPICAM data will be used to study the effects of a dust storm on the mesopause and on thermal tides in the upper atmosphere. This effort will develop strong ties between a US institution and the SPICAM team.

Summary of personnel and effort:

Name	Role	Institution	Funded Effort per year	Unfunded Effort per year
Dr. Paul Withers	PI	Boston Univ.	3 months	0
Dr. Jean-Loup Bertaux	Co-I	Boston Univ.	1.5 months	0
Dr. John Clarke	Co-I	Boston Univ.	0	As needed
Dr. Franck Montmessin	Collaborator	Service d'Aeronomie France	0	As needed
Graduate Student	Graduate Student	Boston Univ	6 months	0

Analysis of SPICAM Stellar Occultation Data

1 - Introduction

The SPICAM UV spectrometer on the Mars Express spacecraft has used stellar occultations to measure >600 vertical profiles of CO₂ number density in the atmosphere of Mars. Corresponding vertical profiles of mass density (ρ), pressure (p), and temperature (T) as functions of altitude have been derived from each of these profiles. We propose to use SPICAM ρ , p , and T profiles to investigate the dynamics and thermal structure of the middle and upper martian atmosphere between 50 km and 150 km (Figs 1 and 2). SPICAM PI Jean-Loup Bertaux has recently been appointed a Senior Research Associate at Boston University.

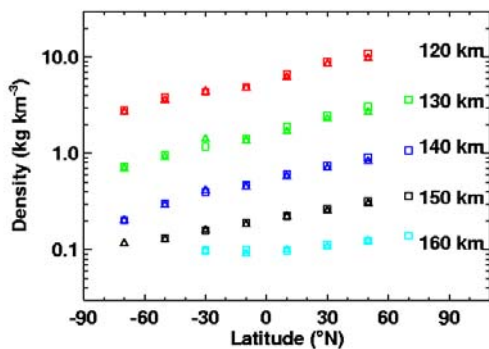
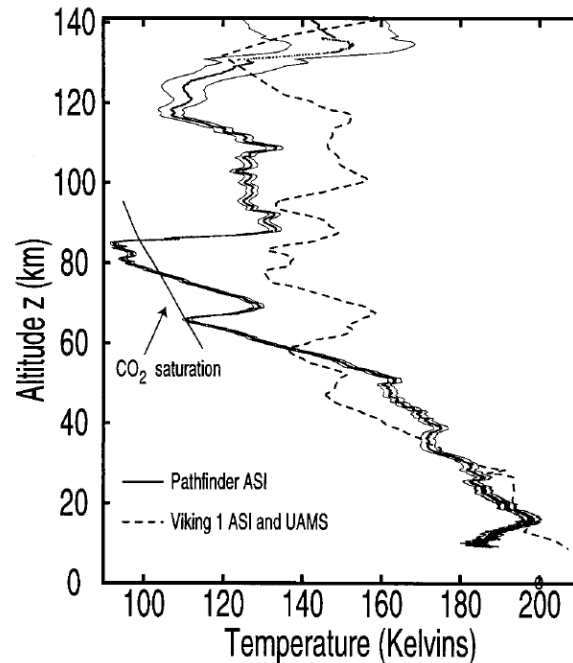


Fig 1 (left). MGS accelerometer density measurements at Ls~60° and local solar time (LST) = 15 hrs. Densities are smallest at the southern winter pole (from Withers, 2006).

Fig 2 (right). Pathfinder (solid line with 1 σ error envelope) and Viking 1 (dashed line) entry profiles. Pathfinder's mesopause temperature is below the freezing point of CO₂. Middle and upper atmospheric thermal structure differs greatly from the lower atmosphere's (from Magalhães et al., 1999).



Raw SPICAM data and extensive calibration information have been peer-reviewed and archived by NASA's Planetary Data System (PDS) and its ESA equivalent (PDS, 2007). All higher-level SPICAM data products can be derived from this archive. The ρ , p , and T profiles are publicly available online at bdap.ipsl.jussieu.fr/ or via sirius.bu.edu/withers/. This proposed effort will be accomplished using publicly available data.

The 50 - 150 km region of the atmosphere is an important part of the Mars system (Barth et al., 1992; Zurek, 1992; Zurek et al., 1992; Magalhães et al., 1999). The expected thermal structure at these altitudes is dominated by the cold mesopause at 80 - 100 km and the transition to the isothermal exosphere around ~180 km (Fig 1; e.g. Bougher et al., 2002). There are few observations of how the mesopause altitude and temperature change

with season (Ls), latitude, and local solar time (LST) (Bougher and Dickinson, 1988; Clancy et al., 2007). The mesopause lies between the lower atmosphere, which is heated by visible solar radiation and infra-red emissions from suspended dust, and the upper atmosphere, which is heated by solar UV/EUV radiation. The global circulation patterns between 50 km and 150 km have not been directly observed. Strong global-scale thermal tides are present, as are smaller-scale gravity waves (Forbes et al., 2002; Withers et al., 2003a; Tolson et al., 2005; Creasey et al., 2006). These vertically-propagating disturbances interact with each other and with the mean circulation, transferring energy and momentum as they move upwards (Forbes, 2002). The 50 km - 150 km region of the atmosphere is important for the ionosphere (100-200 km), the homopause (~120 km), and the transport of light species up into the exosphere (>180 km). Some of the major questions related to this part of the atmosphere are: How variable are the mesopause's altitude and temperature and what causes those variations? What is the global circulation? How does the middle and upper atmosphere respond to dust storms in the lower atmosphere? How are waves/tides in the lower and upper regions of the atmosphere related? Our four tasks (Sections 4-7) involve comparisons of SPICAM, accelerometer, and model data around the mesopause; merger of TES, SPICAM, and accelerometer data to form composite T(p) profiles between 0 and 200 km; the effects of thermal tides at 50-150 km; and the effects of dust storms at 50-150 km.

These atmospheric regions are difficult to observe, so they have not been studied thoroughly. Published radio occultation observations extend from the surface to ~40 km (Hinson et al., 2001). Observations by thermal infra-red spectrometers, such as TES, PFS and their predecessors, are also restricted to the lower atmosphere (Smith et al., 2001; Grassi et al., 2007). The upper atmosphere has been observed by Mariner UV spectrometers (airglow observations) and several recent accelerometer experiments during aerobraking (density measurements along the spacecraft's trajectory) (Stewart et al., 1972; Keating et al., 1998; Withers, 2006; Keating et al., 2007). Five landers have each measured one vertical profile of density, pressure, and temperature during entry (Withers and Smith, 2006, and references therein). Several models exist for the upper atmosphere, including the LMD model based in Paris and Bougher's model at the University of Michigan (Angelats i Coll et al., 2005; Bougher et al., 2006).

2 - SPICAM

SPICAM is a near-IR and UV spectrometer aboard Mars Express (Bertaux et al., 2004). We shall focus on vertical ρ , p , T profiles obtained from SPICAM UV stellar occultations (Fig 3; Quemérais et al., 2006). Analysis of SPICAM ρ , p , T profiles is timely because the dataset is relatively new and unexplored. This work is also timely because it will provide context for studies of anticipated MRO Mars Climate Sounder (MCS) ρ , p , T profiles between 0-80 km (McCleese et al., 2007). The SPICAM dataset will not become worthless once large quantities of MCS data are available. SPICAM samples different altitudes and LSTs. SPICAM data were collected for 2.5 years before MRO reached mapping orbit, giving SPICAM and TES months of simultaneous operation.

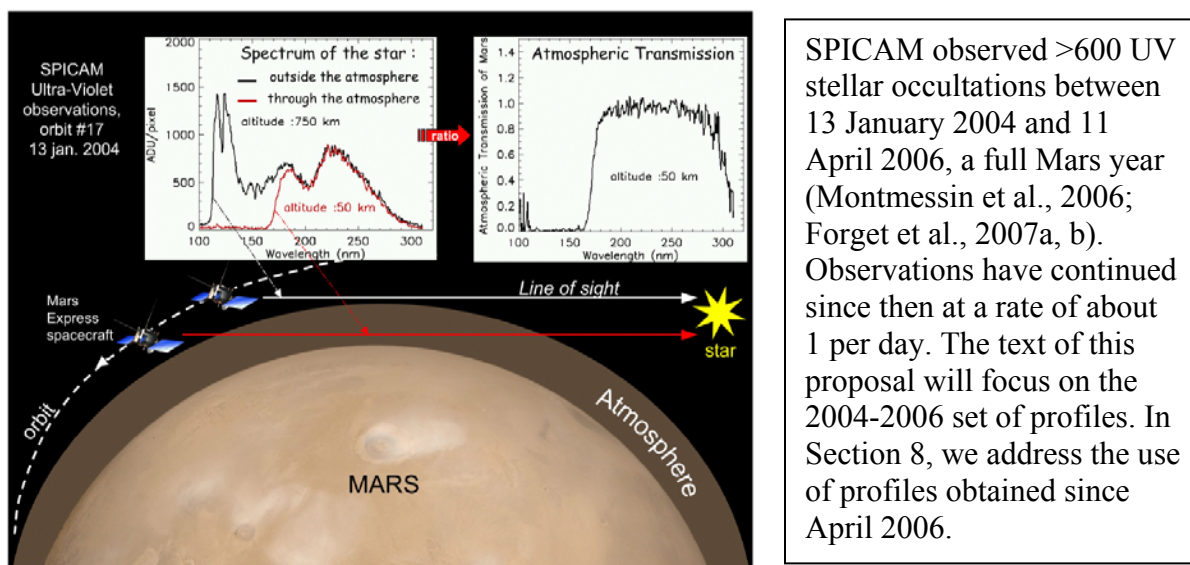


Fig 3. Schematic diagram of a SPICAM stellar occultation (from Bertaux et al., 2006).

Each occultation lasts a few minutes, much shorter than timescales for atmospheric changes. The latitude and longitude of the point of closest approach between the ray path and Mars vary by only a few tens of kilometres during an occultation, much smaller than the horizontal lengthscale ($(\text{scale height} \times \text{planetary radius})^{0.5} \sim 200 \text{ km}$) of the derived atmospheric profile. Typical vertical resolution in the raw data is about 1 km, usually smoothed to a few km, less than half a scale height, in the derived profiles (Fig 4).

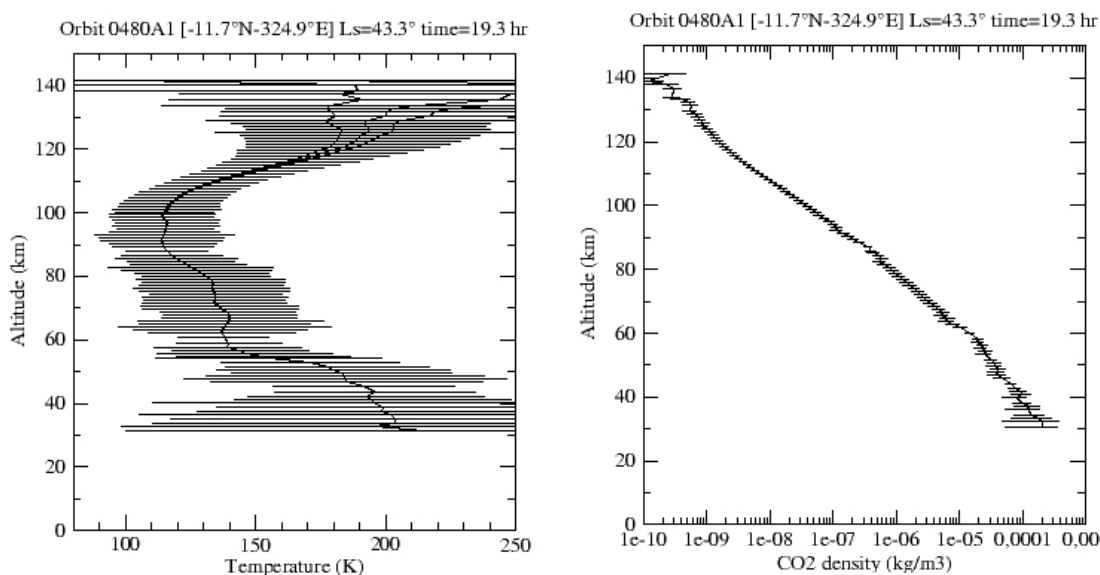


Fig 4. SPICAM temperature and density profiles from orbit 0480A1 (12°S, Ls=43°, LST=19 hrs) with 1σ errors (from Forget et al., 2007b).

The typical vertical range for $\rho(z)$ is 50 - 150 km. The typical vertical range for $p(z)$ and $T(z)$ is 50 - 130 km, reduced from 150 km by uncertainties in the upper boundary condition for the equation of hydrostatic equilibrium (Quemerais et al., 2006). Typical

uncertainties in density and pressure are 20%, typical uncertainty in temperature is 30 K (Quemerais et al., 2006; Forget et al., 2007a, b). Given the >150 K difference between exospheric temperatures of 250 K and mesopause temperatures of <100 K, the 30 K temperature uncertainty is not a problem. Further smoothing can be applied to decrease the temperature uncertainty, at the cost of reduced vertical resolution, if necessary for any task.

Latitude, LST, and Ls coverage are shown in Fig 5. Due to the MEX orbit, latitude/LST coverage in later Mars years will be very similar to the first Mars year's coverage. For instance, there are seven observations in 2004 and seven in 2006 that satisfy $Ls=30^{\circ}-60^{\circ}$, latitude= $40^{\circ}N-50^{\circ}N$, LST = 20-22 hrs. Studies of interannual variability within the SPICAM dataset will be possible (Section 8).

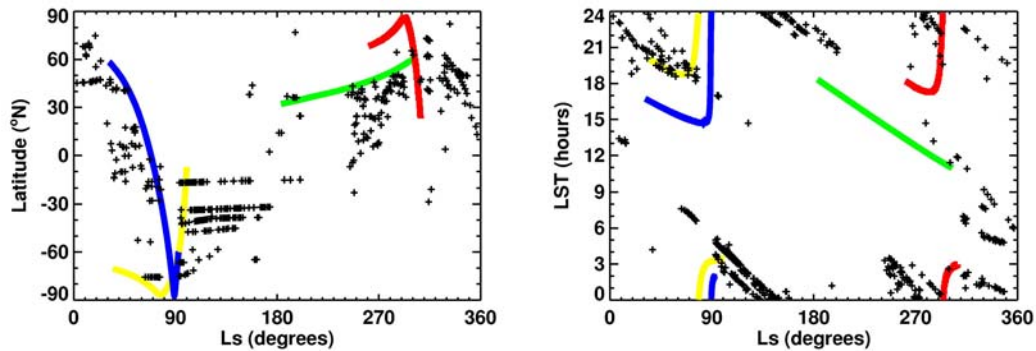


Fig 5. Latitude, Ls, and LST coverage for SPICAM (crosses) and accelerometers (solid lines). MGS Phase 1 = green, MGS Phase 2 = blue, ODY = red, MRO = yellow.

3 - Previous Results from SPICAM ρ , p , T Profiles

The first detailed paper on scientific interpretation of SPICAM stellar occultation results is currently under preparation for submission to JGR (Forget et al., 2007b). It is likely to have been submitted before this proposal is reviewed. Results have been presented at a conference (Forget et al., 2007a). This proposal does not duplicate work that has already been performed by Forget et al. We now summarize their main findings.

Densities varied by a factor of three from perihelion to aphelion at 70 km and by a factor >10 above 100 km. This is consistent with lower atmospheric temperatures increasing by 20 K during a Mars year, as seen by TES (Smith, 2004). Density varied gradually with season, except for around $Ls=130^{\circ}$ when a regional-scale dust storm affected the atmosphere at all altitudes, significantly before the usual season (Smith et al., 2006). Dust storm warming occurred at all altitudes between the surface and 100 km, in contrast to models that predicted that warming is restricted to the lower atmosphere, below ~ 50 km. Comparison between SPICAM observations and the LMD Mars General Circulation Model at all seasons showed that the model underpredicted temperatures by tens of Kelvin at all altitudes above ~ 70 km. Forget et al. (2007b) suggest that errors in how CO_2 radiative cooling is modelled are partially, but not completely, responsible for these errors in the model's predictions.

4 - Task 1: Comparison of SPICAM Data, Accelerometer Data, and Model Predictions

This task involves comparisons between SPICAM profiles, aerobraking accelerometer data, and theoretical simulations. We now describe the available aerobraking data, the available theoretical simulations, and the planned scientific analysis.

MGS, ODY, and MRO measured densities between ~ 100 km and ~ 160 km on >1500 aerobraking passes (Keating et al., 1998; Withers et al., 2003a; Tolson et al., 2005; Withers, 2006). Periapsis latitude, L_s , and LST are shown in Figure 5. MGS data have been peer-reviewed and archived at the PDS (MGS, 2001). A partial ODY dataset has been delivered to the PDS, but not peer-reviewed (Fig 6; ODY, 2004). Withers, who briefly received support from the ODY Participating Scientist program, has completed preliminary processing of the entire raw ODY dataset and derived density profiles for all ODY aerobraking passes (ODY, 2006). MRO density profiles are publicly available from the PDS at ftp://atmos.nmsu.edu/PDS/review/MROA_1001. p , T profiles can be derived from accelerometer vertical ρ profiles using hydrostatic equilibrium and the ideal gas law. Vertical ρ profiles can be generated by averaging inbound and outbound legs of the aerobraking pass. The mean molecular mass, which is needed to obtain T , is available from Bougher (2007). We shall derive p , T profiles from accelerometer ρ profiles as needed by Tasks 1 and 2.

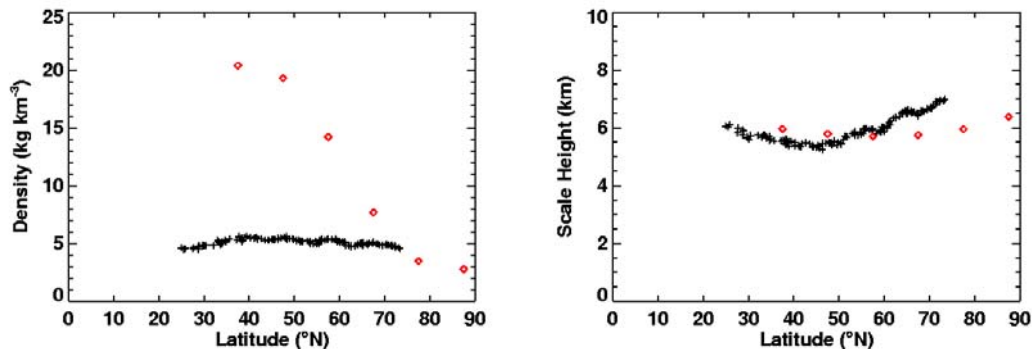


Fig 6. Smoothed ODY accelerometer data at 120 km and LST=03 hrs (black crosses) and model predictions (red diamonds) from Bougher (2007, file MS01DCC.AB2.html).

Temperatures predicted by the LMD Mars General Circulation Model were significantly warmer than SPICAM observations (Section 3; Forget et al., 2007b). This model began as a lower atmosphere model and it has recently been extended to the upper atmosphere (Angelats i Coll et al., 2005). It is possible that its established lower atmospheric modules are working well, but that its new upper atmospheric modules are incomplete. By contrast, Bougher's Mars Thermospheric General Circulation Model (MTGCM) is a dedicated thermospheric model that has been tested and validated for over a decade (Bougher et al., 2006, and references therein). It uses output from the NASA Ames MGCM as its lower boundary (e.g. Haberle et al., 1999). Tabulated MTGCM predictions of ρ , p , T , and μ for altitudes between 90 km and 200 km and conditions appropriate for MGS, ODY, and MRO aerobraking are publicly available online (Fig 6; Bougher, 2007). Many figures in Bougher's publications also display predictions relevant for aerobraking

conditions, such as contour plots of density or temperature as functions of latitude and LST or latitude and altitude (Bougher and Dickinson, 1988; Bougher and Roble, 1991; Bougher et al., 1997, 1999, 2000, 2001, 2002, 2004, 2006).

Table 1 lists 6 cases where SPICAM data, accelerometer data, and MTGCM simulations are available for the same narrow range of Ls, latitude, and LST. SPICAM and accelerometer data come from different Mars years. Interannual variability in the lower atmosphere is small at Ls~100°, but large at Ls~300° (Smith, 2004). We shall first compare zonally-averaged $\rho(z)$, $T(z)$, and $T(p)$ at altitudes where SPICAM and accelerometer data are both available (100 - 150 km) to determine whether interannual variability is significant for any of the 6 cases in Table 1.

Ls	Latitude	LST (hr)	N-SPICAM	N-ACC	Spacecraft
80° - 100°	90°S - 60°S	01 - 05	8	127	MRO
90° - 120°	60°S - 30°S	01 - 05	54	99	MRO
90° - 120°	30°S - 0°	02 - 05	35	57	MRO
290° - 320°	50°N - 70°N	01 - 03	5	63	ODY
90° - 110°	85°S - 65°S	01 - 04	7	49	MGS
276° - 316°	40°N - 65°N	10 - 15	7	61	MGS

Table 1. Cases where SPICAM and accelerometer measurements sample the same Ls, latitude, and LST. N-SPICAM is the number of SPICAM profiles that satisfy the Ls, latitude, and LST constraints. N-ACC is the number of accelerometer profiles whose periapsis satisfies the constraints.

For cases where SPICAM and accelerometer data are similar, we shall compare data and model predictions. For cases where they are dissimilar, we shall see if MTGCM predictions are consistently closest to one dataset or the other. This might occur if the MTGCM uses lower atmospheric dust conditions appropriate for the year of the SPICAM observations, but not for the year of the accelerometer observations, for example.

Model-data comparisons will identify any areas of weakness in the widely-used MTGCM predictions. Fig 6 shows that MTGCM temperature (scale height) predictions are accurate, unlike those of Forget et al. (2007b), suggesting that its thermospheric heating and cooling processes are accurate. However, meridional gradients in MTGCM densities at 120 km are much greater than observed. The MTGCM predictions are similar to MGS observations in Fig 2 of Withers (2006); densities decrease towards the winter pole, but thermospheric temperatures are nearly constant with latitude. The diversity of seasons, latitudes, and LSTs in Table 1 is valuable.

5 - Task 2: Formation and Analysis of Composite T(p) Profiles From Surface to 200 km

TES, SPICAM, and MRO data will be combined to produce composite profiles of atmospheric structure from the surface to 200 km at LST = 02 hrs. TES nadir T(p) profiles extend from the surface to 10 Pa (Withers and Smith, 2006). Combined with TES limb data, they extend to altitudes above the 1 Pa level (Fig 7; Smith et al., 2001). SPICAM profiles extend upwards from the ~4 Pa level (Fig 4, $\rho = 10^{-4} \text{ kg m}^{-3}$, $T = 200$

K; Forget et al., 2007b) to 150 km. MRO results up to 200 km have been presented at meetings, but currently archived data products extend to 150 km only - "Altitude is limited to 150 km until the fuel slosh issue is resolved" (MRO, 2007). Our efforts in this task will depend on MRO data availability (paragraph A or B below).

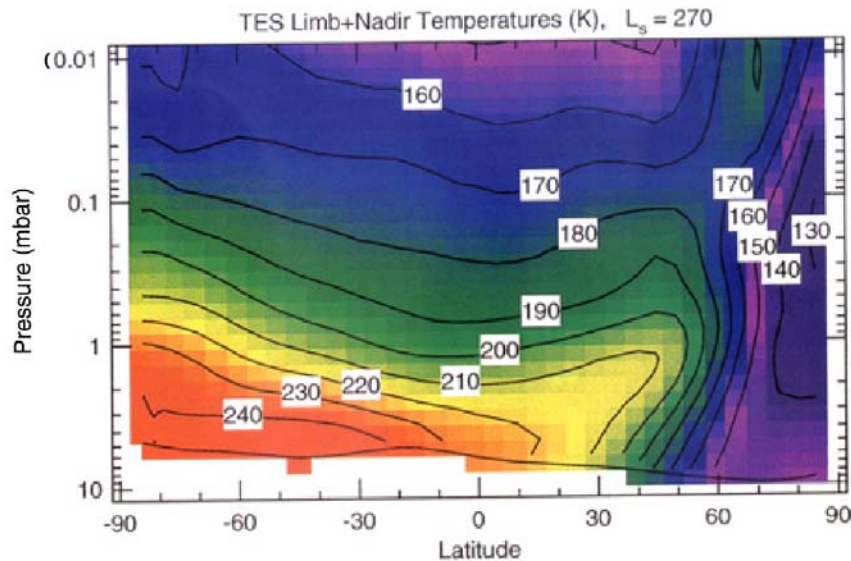


Fig 7. TES limb and nadir temperatures as a function of pressure and latitude (from Smith et al., 2001). 0.01 mbar = 1 Pa.

A) If MRO density profiles up to 200 km are archived:

TES data (2 AM / 2 PM) are available that satisfy the Ls, latitude, LST constraints for all 6 cases in Table 1. Lower atmospheric interannual variability is small for the three cases involving MRO data at Ls~100°. If the upper atmospheric interannual variability is also low for these cases, which seems likely, then we shall derive p and T profiles from the MRO density profiles between 100 km and 200 km (Section 4). We shall then combine TES, SPICAM, and MRO T(p) profiles to form composite T(p) profiles from the surface to 200 km. First, one composite profile for each of the three MRO cases in Table 1 will be produced. Additional profiles with, for example, better latitude resolution than 30° degrees will be produced as permitted by the overlap in Ls, latitude, and LST between TES, SPICAM, and MRO data.

B) If MRO density profiles up to 200 km are not archived:

Over 100 SPICAM profiles have LST between 00 and 04 hours, close to TES 2 AM data, at Ls~120° (Fig 5). SPICAM and TES data are from different Mars years at these seasons, but this is a time of low interannual variability (Smith, 2004). We will not consider SPICAM data after Ls=130°, the onset of an unusual regional dust storm (Section 7). TES limb profiles are recorded every 10° on each MGS orbit (Smith et al., 2001). Lower atmospheric conditions at intermediate latitudes can be found by interpolation. Most SPICAM occultations were restricted to four narrow latitude bands, each of width a few degrees, at this season (Fig 5). We shall divide these >100 SPICAM occultations into 12 subsets (the four narrow latitude bands and Ls=100°-110°, 110°-120°, and 120°-130°). Corresponding TES T(p) profiles will be found, either by averaging or by selection of a typical profile, for each of the 12 latitude/Ls subsets. Composite T(p) profiles from the surface to 150 km will be formed for each of these subsets from TES and SPICAM data. Also, ~20 SPICAM profiles from Ls~330°, 60°N, and LST=01 hrs, a season of low interannual variability, will be combined with TES data to form one

additional composite T(p) profile (Fig 5). High interannual variability at Ls~250° precludes the formation of composite profiles at this season, despite abundant SPICAM 2 AM data (Fig 5).

Regardless of MRO data availability and the choice between paragraphs A and B above, useful composite T(p) profiles from the surface to the thermosphere will be obtained during this task. We shall use them to investigate the vertical thermal structure of the Mars atmosphere at nighttime and Ls~100°. How are lower atmospheric meridional gradients related to those in the upper atmosphere? How do these T(p) profiles compare to the five entry profiles with comparable vertical range (Withers and Smith, 2006)?

If variations in atmospheric properties with Ls and/or latitude are relatively small, then it will be possible to create composite T(p) profiles at specific longitudes, rather than zonally averaging data. Variations in atmospheric properties with longitude due to thermal tides can then be studied from the surface to 150 km or higher, a valuable addition to the results of Task 3.

6 - Task 3: Effects of Thermal Tides in SPICAM Data

Cases where SPICAM profiles cover all longitudes over a narrow range of Ls, latitude, and LST will be used to quantify zonal variations in atmospheric properties due to thermal tides. Many Mars atmospheric observations contain evidence for strong thermal tides, which affect the structure and dynamics of the atmosphere. They are particularly visible as large variations in density with longitude at aerobraking altitudes. We first outline the theory behind thermal tides, following Forbes et al. (2002), and explain why they are important, before describing our specific SPICAM analysis plans.

6.1 - Summary: Thermal Tides

Solar radiation drives atmospheric motions on Mars. Global-scale motions whose periods are related to a sol are referred to as thermal tides. They satisfy similar equations to those that govern gravitational tides in Earth's oceans. They propagate upwards from the surface. Many Mars atmospheric observations contain evidence for strong thermal tides, which affect the structure and dynamics of the atmosphere (e.g. Zurek, 1976; Zurek et al., 1992; Wilson and Hamilton, 1996). A thermal tide can be represented as a Fourier series in time and longitude (Chapman and Lindzen, 1970):

$$A \cos(n\Omega t + s\lambda - \phi_{sn}) \quad (1)$$

where A is amplitude, t is universal time, n is ... -2, -1, 0, 1, 2 ..., s is 1, 2, 3, ..., and ϕ_{sn} is phase. A and ϕ_{sn} are functions of altitude and latitude. s is called the "zonal wavenumber." Each s, n pair forms a unique tidal mode whose values of s and n determine its meridional extent, vertical wavelength, and whether it amplifies or dissipates as it propagates upwards. The incident solar forcing contains only modes with s=n, which move with respect to an observer on the ground at the same speed as the Sun in the sky. They are called "migrating" modes. Solar forcing is dominated by the diurnal and semi-diurnal terms, s=1 or s=2. Universal time, t, and local time, t_{LT} , are related by $\Omega t = \Omega t_{LT} - \lambda$. In terms of t_{LT} , letting n=s, and neglecting amplitude, Eqn 1 becomes:

$$\cos(s\Omega t_{LT} + (s-s)\lambda - \phi_{ss}) \quad (2)$$

Terms like (s-s) will be retained for clarity. If topographical variations are represented by:

$$\cos(m\lambda - \phi_m) \quad (3)$$

Then interactions between solar forcing and zonal variations in topography generate sum-and-difference components that satisfy:

$$\cos(s\Omega t + (s \pm m)\lambda - (\phi_{ss} \pm \phi_m)) \quad (4)$$

$$\cos(s\Omega t_{LT} + ((s-s) \pm m)\lambda - (\phi_{ss} \pm \phi_m)) \quad (5)$$

Whether or not this mode is strongly amplified as it propagates upwards is determined by the pair s, s+/-m (Eqn 4). The zonal wavenumber of this mode in a series of fixed LST observations (eg TES, accelerometer) is ((s-s) +/- m), which reduces to m for all values of s (Eqn 5). So a wave-1 zonal harmonic in a series of fixed LST observations could be formed by any of the following modes:

$$\cos(1\Omega t - (\phi_{11} - \phi_1)) \quad (6)$$

$$\cos(1\Omega t + 2\lambda - (\phi_{11} + \phi_1)) \quad (7)$$

$$\cos(2\Omega t + 1\lambda - (\phi_{22} - \phi_1)) \quad (8)$$

$$\cos(2\Omega t + 3\lambda - (\phi_{22} + \phi_1)) \quad (9)$$

The variations in amplitude and phase with altitude for each of these four modes are different (Withers et al., 2003a, and references therein). If either of the two diurnal modes (Eqns 6-7) are observed at two LSTs 12 hours apart, longitudes that have positive amplitudes at one time will have negative amplitudes at the other time and vice versa. By contrast, if either of the two semi-diurnal modes (Eqns 8-9) are observed at two LSTs 12 hours apart, longitudes that have positive amplitudes at one time will have positive amplitudes at the other time as well. So SPICAM observations at two different LSTs can be used to identify a thermal tide as diurnal or semidiurnal.

Variations in atmospheric observations at fixed LST with longitude will be studied in Task 3. Changes in amplitude and phase of each zonal harmonic with altitude and/or LST will be quantified (Withers et al., 2003a). These results can be studied in two ways. First, to identify the underlying tidal modes present in the martian atmosphere. Second, to constrain conditions in the atmospheric regions through which the tide has propagated. Large-scale characteristics, such as where the tidal mode amplifies as it propagates upwards, where it dissipates, what its e-folding distance for amplitude changes is, and whether its phase shift from 60 km to 120 km is large or small are sufficient to identify the tidal mode (e. g. Forbes et al., 2002; Withers et al., 2003a). The details of those changes depend on atmospheric properties, such as zonal winds and temperatures, so modellers can state, for example, that the observations are consistent with westward, not eastward, zonal winds (e. g. Forbes et al., 2002).

It is important to understand which tidal modes are present in the middle and upper regions of the atmosphere because they play a major role in the general circulation of the atmosphere and are a source of heating where they dissipate. Migrating tides have large amplitudes at low altitudes, but dissipate quickly as they propagate upwards. Lower atmosphere observations (0-40 km) are dominated by migrating tides (Fig 9; Banfield et al., 2000, 2003). Non-migrating tides have small amplitudes at low altitudes, but some of

them amplify as the propagate upwards. Upper atmospheric observations (100-140 km) are dominated by non-migrating tides (Fig 8; Withers et al., 2003a). These non-migrating tides break and dissipate around 160 km, eliminating zonal variations in the atmosphere. SPICAM data span the critical region where non-migrating tides become dominant over migrating tides.

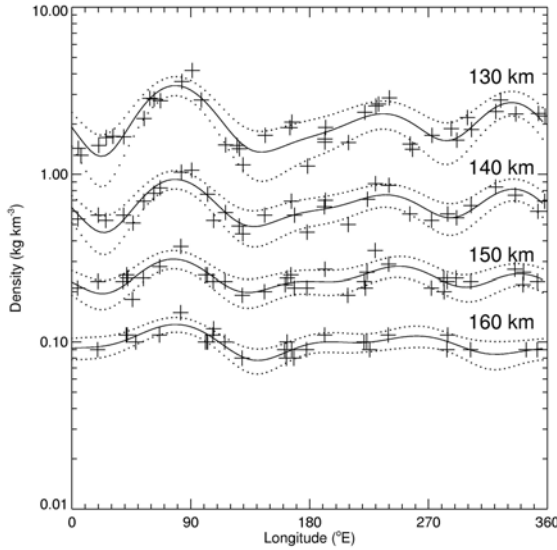
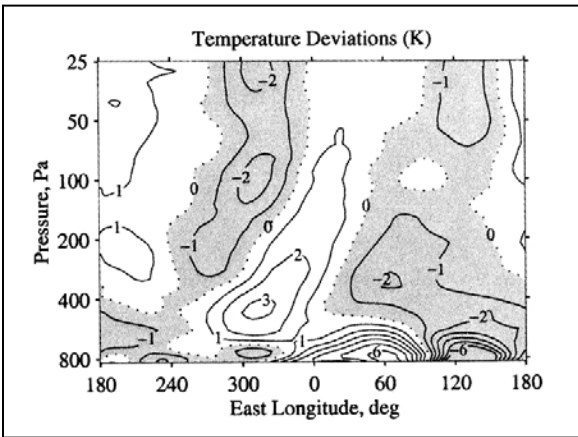


Fig 8 (left). MGS densities between 10°N and 20°N, $L_s \sim 60^\circ$, LST=15 hrs. Densities at 130, 140, 150, 160 km are shown as crosses. Solid lines are model fits and dotted lines are 1σ uncertainties on each fit. Density variations due to thermal tides are present. Tidal amplitudes decrease as altitude increases. Longitudes of density peaks do not vary with altitude, so phases do not vary with altitude (from Withers et al., 2003a).

Fig 9 (right). MGS Radio Science temperature data. Temperature deviations from the zonal mean as a function of pressure and longitude. A mix of harmonics is present at low altitudes, but a wave-2 harmonic becomes dominant by 50 Pa (from Hinson et al., 2001)



6.2 - Description of Task 3

Ls	Latitude	LST (hrs)	N-SPICAM
0° - 50°	40°N - 50°N	19.8 - 23.6	21
30° - 80°	30°S - 20°N	18 - 22	38
90° - 120°	20°S - 10°S	2.6 - 4.8	35
90° - 120°	50°S - 30°S	1.2 - 4.3	52
120° - 150°	50°S - 30°S	22.9 - 2.3	60
150° - 180°	40°S - 30°S	22 - 24	15
240° - 270°	15°N - 45°N	0.8 - 3.5	29
270° - 300°	32°N - 52°N	22.2 - 2.1	26
328° - 348°	38°N - 63°N	4.7 - 5.7	16
325° - 350°	46.7°N - 56.7°N	00 - 02	14

Table 2. Cases where there are many SPICAM profiles in narrow Ls, latitude, and LST ranges that cover all longitudes.

Table 2 lists 10 instances where SPICAM data can be used to study thermal tides. We shall use them to discover how the large zonal variations in $\rho(z)$ seen in accelerometer data from 100 - 160 km (Fig 8) are expressed at lower altitudes of 50-100 km.

Accelerometer data consistently show strong tides in the tropics, so we are confident that tides will be visible in the SPICAM data. If not, we shall place upper limits on tidal amplitudes. The amplitude and phase of each zonal harmonic (up to wavenumber~4) will be determined as a function of altitude for each case in Table 2. The techniques outlined in Section 6.1 and applied in Withers et al. (2003a) will be used to identify the tidal modes present in the middle and upper atmosphere (Withers et al., 2003a).

We predict that zonal variations in $\rho(z)$ will differ from zonal variations in $T(z)$. Suppose densities at 90°E and 130 km are much larger than densities at 180°E and 100 km due to thermal tides and that the zonal variations have completely dissipated by 150 km. The average scale height at 90°E must be smaller than at 180°E. Densities are greater than the zonal mean and temperatures are less than the zonal mean at 90°E. Densities are less than the zonal mean and temperatures are greater than the zonal mean at 180°E. Zonal variations in density and temperature will therefore be anti-correlated in altitude regions where the tides dissipate. Conversely, they will be correlated in altitude regions where the tides amplify. We shall test whether these predictions are accurate. This reasoning suggests that amplitudes and phases of tidal modes in $\rho(z)$ data may appear different in $T(p)$ data, which we shall investigate. This is important because accelerometer data provides $\rho(z)$, but many predictions are given as $T(p)$.

7 - Task 4: Effects of Dust Storms on SPICAM Data

How do the middle and upper regions of the atmosphere respond during a dust storm? MGS accelerometer observations showed rapid and significant changes in densities at 160 km thousands of km away from a regional dust storm (Keating et al., 1998). Forget et al. (2007b) presented SPICAM data showing changes in densities and temperatures during a regional dust storm. The atmospheric profile measured during Spirit's entry, when the equatorial atmosphere was relatively dusty, is the only one of five Mars entry profile that does not contain large amplitude, long wavelength oscillations around the 1 Pa level (60 km) (Withers and Smith, 2006). It is clear that the middle and upper regions of the atmosphere change significantly during a dust storm.

TES ceased regular global atmospheric observations in August 2004 (Fig 10; $L_s=81^\circ$). THEMIS nadir observations monitor dust opacity and atmospheric brightness temperature (Smith et al., 2003). Also, regular measurements of dust opacity above the Spirit and Opportunity Rovers by Mini-TES are available for the entire period of SPICAM observations (Fig 11; Smith et al., 2006). These show that a period of low dust loading ($\tau\sim 0.2$) after $L_s=30^\circ$ ended abruptly at $L_s=130^\circ$ with τ increasing to unity above both rovers in a few sols. This is significantly earlier than the typical start of dust storm season around $L_s\sim 200^\circ$. Optical depth decreased slowly to 0.2, with a timescale of a couple of months, before increasing again to near unity at $L_s\sim 220^\circ$.

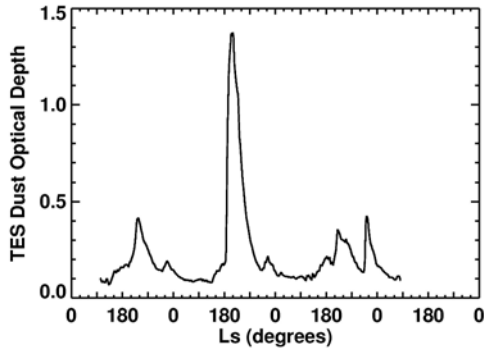
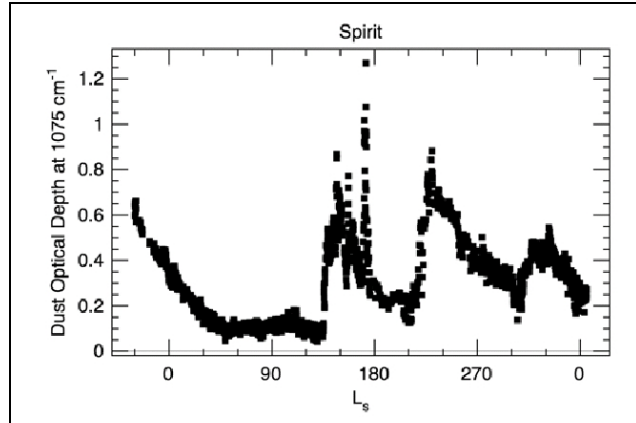


Fig 10 (left). Global-average TES dust optical depth as function of season from Mars Year 24-27 (1998-2004). Conditions are repeatable at $L_s \sim 100^\circ$, but not at $L_s \sim 200^\circ$ - 300° . (Data provided by Mike Smith).

Fig 11 (right). Mini-TES dust optical depth for Spirit (Mars Year 26-28, 2004-2006). The end of the TES dataset overlaps with the beginning of the Mini-TES dataset (from Smith et al., 2006). The large increase in optical depth at $L_s=130^\circ$ in MY 27 did not occur in MY 24-26.



There are 100 SPICAM profiles between $L_s=100^\circ$ and $L_s=130^\circ$ and 60 SPICAM profiles between $L_s=130^\circ$ and $L_s=160^\circ$, but only 20 SPICAM profiles between $L_s=190^\circ$ and 250° . We will therefore concentrate on the $L_s=130^\circ$ dust storm. SPICAM data coverage is very repeatable at this season (Fig 5). Nearly all profiles are between 15°S and 50°S , close to Spirit's and Opportunity's equatorial latitudes. LST changes slowly and monotonically from 04 hours at $L_s=100^\circ$ to 23 hours at $L_s=160^\circ$.

Forget et al. (2007b) presented SPICAM data to show that densities increased at all altitudes at dust storm onset and that warming occurred up to 100 km. We shall compare profiles from (A) before the $L_s=130^\circ$ dust storm, (B) from the period immediately after dust storm onset, and (C) in the waning phase of the dust storm. Oscillations in $T(z)$ or $T(p)$ entry profiles have been attributed to tides (Magalhães et al., 1999). Dust storms are known to amplify some tidal modes, and we will determine how the amplitude and wavelength of oscillations in $T(z)$ or $T(p)$ changed (e. g. Zurek and Leovy, 1981, Bridger and Murphy, 1998). How do variations in atmospheric properties with longitude due to thermal tides change from the pre-dust storm phase to the waning phase of the dust storm? Dust storms heat the lower atmosphere and make the lower atmosphere nearly isothermal (Zurek, 1992). Does warming occur at all altitudes simultaneously or does the upper atmosphere warm more slowly? What are the effects on the temperature minimum at the mesopause? We shall address these questions, which were not answered by Forget et al. (2007b).

8 - Impact of Additional SPICAM Data and MCS Data

SPICAM data from after April 2006 will become publicly available before the end of this proposed work. They will be useful for several of the above tasks. Data from April -

August 2006, the time of MRO aerobraking, will remove problems of interannual variability from parts of Task 1. There will be more groups of occultations that are tightly clustered in Ls, LST, and latitude, which will benefit Task 3. Observations during multiple dust storm seasons will be useful in Task 4, because lower atmospheric conditions at this season vary so much from year to year. MCS ρ , p, T profiles are not yet publicly available. If they become available during this effort, they will be used to support the proposed tasks.

9 - Anticipated Results and Broader Implications

Successful completion of this project will provide new studies on coupling between the lower and upper regions of the martian atmosphere. Interactions between data analysis efforts and modeling efforts are essential for ensuring that models are consistent with reality and that the power of numerical models to explore unobserved parameter space enhances the data interpretation. Although this project does not include any theorists who model the martian atmosphere (which streamlines project management), we will ensure that our results are disseminated in ways that make them useful to theorists and encourage theorists to reproduce them. As our data analysis tasks are completed, their results will be presented at conferences and published. There are so few data available to validate models in the 50 - 100 km region of the atmosphere that the results of our data analysis will inevitably pose challenges for theorists.

The SPICAM dataset will be an integral dataset for Mars atmospheric research for many years into the future. We anticipate that studies such as MCS/SPICAM comparisons, interannual variability within the SPICAM dataset, long-term trends in auroral observations, middle and upper atmospheric response to different types of dust storms, and solar cycle effects on the thermosphere will be enhanced by the SPICAM dataset for the next decade. SPICAM data will be extremely relevant for scientists and engineers planning the future Mars Scout atmospheric science orbiter (Maven or The Great Escape). However, the US scientific community has not made extensive use of SPICAM data. SPICAM Co-Is Stern and Sandel are not leading major research efforts using SPICAM data, although they are co-authors on several papers with lengthy author lists (Bertaux et al., 2000, 2004, 2005a, b, c; Quemerais et al., 2006). Space physicists from Berkeley and SWRI are co-authors on a paper relating magnetospheric electrons to auroral UV emissions (Leblanc et al., 2006). We are not aware of any other publications by US authors using SPICAM data. The only grant currently funded by MDAP or Planetary Atmospheres related to SPICAM data is an MDAP grant to Slanger for airglow studies (MDAP 2006 selections have not yet been listed online). This proposal will develop strong links between several scientists at a US institution and the SPICAM team.

10- Relevance to NASA Programs

This effort addresses NASA Strategic Sub-goals 3B and 3C (Table 1 of the ROSES NRA). This effort is relevant to MEPAG Goal II (Understanding the processes and history of climate on Mars), Objective A (Characterize Mars's atmosphere), Investigation 1 (Determine the present state of the neutral/ionized upper atmosphere). This effort is

directly related to the scientific objectives of the 2011 Mars Scout orbiter - processes affecting the upper atmospheric reservoir available for escape.

11 - Personnel

This project will be performed by PI Withers, Co-Is Bertaux and Clarke, Collaborator Montmessin, and a Boston University graduate student.

PI Withers will be responsible for the management of this project. He will coordinate communication between personnel, monitor progress, and assign tasks. He has published recent papers on the structure and dynamics of the martian atmosphere using accelerometer data (Withers et al., 2003a; Withers, 2006). This proposal includes an application by PI Withers for an Early Career Fellowship. Withers received his PhD in 2003. In addition to a strong publication record, Withers has served on NASA/NSF review panels, reviewed PDS datasets, been a Huygens Science Team member, and been a member of Spirit's Atmospheric Advisory Group for Landing.

Co-I Jean-Loup Bertaux is PI on SPICAM and other spacecraft instruments (SOHO SWAN, Venus Express SPICAV). He is therefore an expert on SPICAM instrument performance and characteristics and has participated in many investigations of the middle and upper martian atmosphere. Bertaux has recently been appointed a Senior Research Associate at Boston University. He will spend part of each year in Boston and part in France. His travel between Boston and France will be supported by other funds.

Co-I John Clarke, Professor in Boston University's Astronomy Department, has collaborated with Bertaux for many years (Bertaux and Clarke, 1989; Clarke et al., 1995). He has also analysed HST UV observations of the Mars atmosphere. He will be the graduate student's academic supervisor. His effort will be supported by his faculty position at Boston University.

The Boston University Astronomy Department's PhD program has >40 graduate students. ~8 students typically arrive each year. We anticipate that a first or second year graduate student will start work on this project. PI Withers and Co-I Clarke will jointly direct the student's effort.

Collaborator Franck Montmessin has worked extensively with SPICAM data and other Mars atmosphere research projects (Montmessin et al., 2002, 2004, 2006). He was responsible for processing the SPICAM ρ , p , T profiles that will be used in this effort. He will provide advice on the quality and other characteristics of the SPICAM data.

This project, which involves multiple people and multiple countries, needs a clear management plan. There will be multiple face-to-face meetings between personnel each year, augmented by telephone and email discussions. It is planned that Bertaux will make two extended visits to Boston each year during his 1.5 m of effort per year. The graduate student will also make one visit to Europe each year to meet with Bertaux, Montmessin, and other SPICAM team members. At other times of the year, all personnel except

Montmessin will participate in biweekly telecons. Montmessin has a relatively small role, so will only need to participate in these telecons occasionally. Results and manuscripts will also be discussed via email. The personnel will also discuss this project when they travel to scientific conferences supported by other grants.

12 - Work Plan

Year 1 (Task 1). Graduate Student will collect and organise the SPICAM, accelerometer, and MTGCM data. Withers and Graduate Student will determine interannual variability using SPICAM and accelerometer data. Withers, Graduate Student, and Bertaux will compare SPICAM, accelerometer, and MTGCM data, then interpret the results.

Year 2 (Task 3). Withers will determine the amplitude and phase of zonal harmonics in SPICAM ρ , p , T profiles using existing software. Graduate Student, supported by Withers, will use these results to identify dominant tidal modes and to investigate predicted anti-correlations in density and temperature. Withers, Graduate Student, and Bertaux will compare the results with previous lower and upper atmospheric tidal observations.

Year 3 (Task 2). Graduate Student will collect and organise appropriate TES and SPICAM data. Withers and Bertaux will decide how to average multiple SPICAM or TES profiles together and how to accurately combine an averaged SPICAM profile with an averaged TES profile. Withers, Graduate Student, and Bertaux will compare the results to predictions and entry profiles.

Year 3 (Task 4). Graduate Student will collect relevant dust data. Withers will perform the stated tidal analyses and Graduate Student will perform the other analyses.

Tasks 2 and 4 are delayed until Year 3 to maximize the chances of MRO accelerometer data being available at 200 km and to allow time for further processing and analysis of THEMIS dust data.

References

Angelats i Coll, M., Forget, F., López-Valverde, M. A., and González-Galindo, F. (2005) The first Mars thermospheric general circulation model: The martian atmosphere from the ground to 240 km, *Geophys. Res. Lett.*, 32, L04201, doi:10.1029/2004GL021368.

Banfield, D., Conrath, B., Pearl, J. C., Smith, M. D., and Christensen, P. (2000) Thermal tides and stationary waves on Mars as revealed by Mars Global Surveyor thermal emission spectrometer, *J. Geophys. Res.*, 105, 9521-9537.

Banfield, D., Conrath, B. J., Smith, M. D., Christensen, P. R., and Wilson, R. J. (2003) Forced waves in the martian atmosphere from MGS TES nadir data, *Icarus*, 161, 319-345.

Barth, C. A., Stewart, A. I. F., Bougher, S. W., Hunten, D. M., Bauer, S. J., and Nagy, A. F. (1992) Aeronomy of the current martian atmosphere, in *Mars*, eds. Kieffer, H. H., Jakosky, B. M., Snyder, C. W., and Matthews, M. S., University of Arizona Press, pp. 1054-1089.

Bertaux, J.-L., and Clarke, J. C. (1989) Deuterium content of the Venus atmosphere, *Nature*, 338, 567-568.

Bertaux, J.-L., and 26 colleagues (2000) The study of the martian atmosphere from top to bottom with SPICAM light on Mars Express, *Planet. Space Sci.*, 48, 1303-1320.

Bertaux, J.-L., and Montmessin, F. (2001) Isotopic fractionation through water vapor condensation: The deuteropause, a cold trap for deuterium in the atmosphere of Mars, *J. Geophys. Res.*, 106, 32879-32884.

Bertaux, J.-L. and 27 colleagues (2004) SPICAM: Studying the global structure and composition of the martian atmosphere, *ESA Special Publication 1240*, 95-120, available online at sci.esa.int/science-e/www/object/doc.cfm?fobjectid=34882

Bertaux, J.-L. and 28 colleagues (2005) Global structure and composition of the martian atmosphere with SPICAM on Mars Express, *Adv. Space Res.*, 35, 31-36.

Bertaux, J.-L. and 10 colleagues (2005) Nightglow in the upper atmosphere of Mars and implications for atmospheric transport, *Science*, 307, 566-569.

Bertaux, J.-L., Leblanc, F., Witasse, O., Quemérais, E., Lilenstein, J., Stern, S. A., Sandel, B., and Korablev, O. (2005) Discovery of an aurora on Mars, *Nature*, 435, 790-794.

Bertaux, J.-L. and 15 colleagues (2006) SPICAM on Mars Express: Observing modes and overview of UV spectrometer data and scientific results, *J. Geophys. Res.*, 111, E10S90, doi:10.1029/2006JE002690.

- Bougher, S. W., and Dickinson, R. E. (1988) Mars mesosphere and thermosphere. I - Global mean heat budget and thermal structure, *J. Geophys. Res.*, 93, 7325-7337.
- Bougher, S. W., and Roble, R. G. (1991) Comparative terrestrial planet thermospheres 1. Solar cycle variation of global mean temperatures, *J. Geophys. Res.*, 96, 11045-11055.
- Bougher, S. W., Murphy, J., Haberle, R. M. (1997) Dust storm impacts on the Mars upper atmosphere, *Adv. Space Res.*, 19, 1255-1260.
- Bougher, S. W., Engel, S., Roble, R. G., and Foster, B. (1999) Comparative terrestrial planet thermospheres 2. Solar cycle variation of global structure and winds at equinox, *J. Geophys. Res.*, 104, 16591-16611.
- Bougher, S. W., Engel, S., Roble, R. G., and Foster, B. (2000) Comparative terrestrial planet thermospheres 3. Solar cycle variation of global structure and winds at solstices, *J. Geophys. Res.*, 105, 17669-17692.
- Bougher, S., Engel, S., Hinson, D., and Forbes, J. (2001) Mars Global Surveyor radio science electron density profiles: Neutral atmosphere implications, *Geophys. Res. Lett.*, 28, 3091-3094.
- Bougher, S. W., Roble, R. G., and Fuller-Rowell, T. (2002) Simulations of the upper atmospheres of the terrestrial planets, in *Atmospheres in the Solar System: Comparative Aeronomy*, *Geophys. Monogr. Ser.*, 130, eds. M. Mendillo, A. Nagy, J. H. Waite, AGU, Washington, DC.
- Bougher, S. W., Engel, S., Hinson, D. P., and Murphy, J. R. (2004) MGS Radio Science electron density profiles: Interannual variability and implications for the martian neutral atmosphere, *J. Geophys. Res.*, 109, E03010, doi:10.1029/2003JE002154.
- Bougher, S. W., Bell, J. M., Murphy, J. R., Lopez-Valverde, M. A., and Withers, P. (2006) Polar warming in the Mars thermosphere: Seasonal variations owing to changing insolation and dust distributions, *Geophys. Res. Lett.*, 33, L02203, doi:10.1029/2005GL024059.
- Bougher, S. W. (2007) http://data.engin.umich.edu/tgcm_planets_archive/index.html
- Bridger, A. F. C., and Murphy, J. R. (1998) Mars' surface pressure tides and the behavior during global dust storms, *J. Geophys. Res.*, 103, 8587-8601.
- Chapman, S., and Lindzen, R. S. (1970) *Atmospheric Tides*, Gordon and Breach, New York.
- Clancy, R. T., Wolff, M. J., Whitney, B. A., Cantor, B. A., and Smith, M. D. (2007) Mars equatorial mesospheric clouds: Global occurrence and physical properties from Mars

Global Surveyor Thermal Emission Spectrometer and Mars Orbiter Camera observations, *J. Geophys. Res.*, 112, E04004, doi:10.1029/2006JE002805.

Clarke, J. C., Lallement, R., Bertaux, J.-L., and Quemerais, E. (1995) HST/GHRS observations of the interplanetary medium downwind and in the inner solar system, *Astrophys. J.*, 448, 893-904.

Creasey, J. E., Forbes, J. M., and Keating, G. M. (2006) Density variability at scales typical of gravity waves observed in Mars' thermosphere by the MGS accelerometer, *Geophys. Res. Lett.*, 33, L22814, doi:10.1029/2006GL027583.

Forbes, J. M. (2002) Wave coupling in terrestrial planet atmospheres, in *Atmospheres in the Solar System: Comparative Aeronomy*, *Geophys. Monogr. Ser.*, 130, eds. M. Mendillo, A. Nagy, J. H. Waite, AGU, Washington, DC, pp. 171-190.

Forbes, J. M., Bridger, A. F. C., Bougher, S. W., Hagan, M. E., Hollingsworth, J. L., Keating, G. M., and Murphy, J. R. (2002) Nonmigrating tides in the thermosphere of Mars, *J. Geophys. Res.*, 107, 5113, doi:10.1029/2001JE001582.

Forget, F., Lebonnois, S., Angelats i Coll, M., Quemerais, E., Bertaux, J.-L., Montmessin, F., Dimarellis, E., Reberac, A., Lopez-Valverde, M. A., and Gonzalez-Galindo, F. (2007a) Mars atmosphere density and temperature between 50 and 130 km observed by Mars Express SPICAM stellar occultation, 7th International Conference on Mars, abstract 3029.

Forget, F., Lebonnois, S., Gonzalez-Galindo, F., Quemerais, E., Bertaux, J.-L., Montmessin, F., Reberac, A., and Lopez-Valverde, M. A. (2007b) The density and temperatures of the upper martian atmosphere measured by stellar occultations with Mars Express SPICAM, in preparation for submission to *J. Geophys. Res.*

Grassi, D., Formisano, V., Forget, F., Fiorenza, C., Ignatiev, N. I., Maturilli, A., and Zasova, L. V. (2007) The martian atmosphere in the region of Hellas basin as observed by the planetary Fourier spectrometer (PFS-MEX), *Planet. Space Sci.*, 55, 1346-1357.

Haberle, R. M., Joshi, M. M., Murphy, J. R., Barnes, J. R., Schofield, J. T., Wilson, G., Lopez-Valverde, M., Hollingsworth, J. L., Bridger, A. F. C., and Schaeffer, J. (1999) General circulation model simulations of the Mars Pathfinder atmospheric structure investigation/meteorology data, *J. Geophys. Res.*, 104, 8957-8974.

Hinson, D. P., Tyler, G. L., Hollingsworth, J. L., and Wilson, R. J. (2001) Radio occultation measurements of forced atmospheric waves on Mars, *J. Geophys. Res.*, 106, 1463-1480.

Keating, G. M., and 27 colleagues (1998) The structure of the upper atmosphere of Mars: In situ accelerometer measurements from Mars Global Surveyor, *Science*, 279, 1672-1676.

Keating, G. M., Bougher, S. W., Theriot, M. E., Tolson, R. H., Zurek, R. W., Blanchard, R. C., Murphy, J. R., and Bertaux, J.-L. (2007) Mars neutral upper atmosphere temporal and spatial variations discovered from the accelerometer science experiment aboard Mars Reconnaissance Orbiter, 38th Lunar and Planetary Science Conference, abstract 2074.

Leblanc, F., Witasse, O., Winningham, J., Brain, D., Lilenstein, J., Blelly, P.-L., Frahm, R. A., Halekas, J. S., and Bertaux, J.-L. (2006) Origins of the martian aurora observed by Spectroscopy for Investigation of Characteristics of the Atmosphere of Mars (SPICAM) on board Mars Express, *J. Geophys. Res.*, 111, A09313, doi:10.1029/2006JA011763.

Magalhães, J. A., Schofield, J. T., and Seiff, A. (1999) Results of the Mars Pathfinder atmospheric structure investigation, *J. Geophys. Res.*, 104, 8943-8955.

McCleese, D. J. and 14 colleagues (2007) High vertical and temporal resolution observations of the martian atmosphere, 7th International Conference on Mars, abstract 3252.

MGS (2001) http://pds-atmospheres.nmsu.edu/PDS/data/mgsa_0002/

Montmessin, F., Rannou, P., and Cabane, M. (2002) New insights into martian dust distribution and water-ice cloud microphysics, *J. Geophys. Res.*, 107, 5037, doi:10.1029/2001JE001520.

Montmessin, F., Forget, F., Rannou, P., Cabane, M., and Haberle, R. M. (2004) Origin and role of water ice clouds in the martian water cycle as inferred from a general circulation model, *J. Geophys. Res.*, 109, E10004, doi:10.1029/2004JE002284.

Montmessin, F., Quemérais, E., Bertaux, J.-L., Korablev, O., Rannou, P., and Lebonnois, S. (2006) Stellar occultations at UV wavelengths by the SPICAM instrument: Retrieval and analysis of martian haze profiles, *J. Geophys. Res.*, 111, E09S09, doi:10.1029/2005JE002662.

MRO (2007)

http://atmos.nmsu.edu/PDS/review/MROA_1001/DATA/LEVEL3/P100_199/P100/L3P100.TAB

ODY (2004) http://pds-atmospheres.nmsu.edu/data_and_services/atmospheres_data/odyssey_data.htm

ODY (2006) http://sirius.bu.edu/witthers/odyaccresultsformro_v1point0/

PDS (2007) http://pds-geosciences.wustl.edu/missions/mars_express/spicam.htm

Quemérais, E., Bertaux, J.-L., Korabiev, O., Dimarellis, E., Cot, C., Sandel, B. R., and Fussen, D. (2006) Stellar occultations observed by SPICAM on Mars Express, *J. Geophys. Res.*, 111, E09S04, doi:10.1029/2005JE002604.

Smith, M. D., Pearl, J. C., Conrath, B. J., and Christensen, P. R. (2001) Thermal Emission Spectrometer results: Mars atmospheric thermal structure and aerosol distribution, *J. Geophys. Res.*, 106, 23929-23945.

Smith, M. D., Bandfield, J. L., Christensen, P. R., and Richardson, M. I. (2003) Thermal Emission Imaging System (THEMIS) infrared observations of atmospheric dust and water ice cloud optical depth, *J. Geophys. Res.*, 108, 5115, doi:10.1029/2003JE002115.

Smith, M. D. (2004) Interannual variability in TES atmospheric observations of Mars during 1999-2003, *Icarus*, 167, 148-165.

Smith, M. D., Wolff, M. J., Spanovich, N., Ghosh, A., Banfield, D., Christensen, P. R., Landis, G. A., and Squyres, S. W. (2006) One martian year of atmospheric observations using MER Mini-TES, *J. Geophys. Res.*, 111, E12S13, doi:10.1029/2006JE002770.

Stewart, A. I., Barth, C. A., Hord, C. W., and Lane, A. L. (1972) Mariner 9 ultraviolet spectrometer experiment: Structure of Mars's upper atmosphere, *Icarus*, 17, 469-474.

Tolson, R. H., Dwyer, A. M., Hanna, J. L., Keating, G. M., George, B. E., Escalera, P. E., and Werner, M. R. (2005) Application of accelerometer data to Mars Odyssey aerobraking and atmospheric modeling, *J. Spacecr. Rockets*, 42, 435-443.

Wilson, R. J., and Hamilton, K. (1996) Comprehensive model simulation of thermal tides in the martian atmosphere, *J. Atmos. Sci.*, 53, 1290-1326.

Withers, P., Bougher, S. W., and Keating, G. M. (2003a) The effects of topographically-controlled thermal tides on the martian upper atmosphere as seen by the MGS accelerometer, *Icarus*, 164, 14-32.

Withers, P., Towner, M. C., Hathi, B., and Zarnecki, J. C. (2003b) Analysis of entry accelerometer data: A case study of Mars Pathfinder, *Planet. Space Sci.*, 51, 541-561.

Withers, P. (2006) Mars Global Surveyor and Mars Odyssey accelerometer observations of the martian upper atmosphere during aerobraking, *Geophys. Res. Lett.*, 33, L02201, doi:10.1029/2005GL024447.

Withers, P., and Smith, M. D. (2006) Atmospheric entry profiles from the Mars Exploration Rovers Spirit and Opportunity, *Icarus*, 185, 133-142.

Zurek, R. W. (1976) Diurnal tide in the martian atmosphere, *J. Atmos. Sci.*, 33, 321-337.

Zurek, R. W., and Leovy, C. B. (1981) Thermal tides in the dusty martian atmosphere: A verification of theory, *Science*, 213, 437-439.

Zurek, R. W. (1992) Comparative aspects of the climate of Mars: An introduction to the current atmosphere, in *Mars*, eds. Kieffer, H. H, Jakosky, B. M., Snyder, C. W., and Matthews, M. S., University of Arizona Press, pp. 799-817.

Zurek, R. W., Barnes, J. R., Haberle, R. M., Pollack, J. B., Tillman, J. E., and Leovy, C. B. (1992) Dynamics of the atmosphere of Mars, in *Mars*, eds. Kieffer, H. H, Jakosky, B. M., Snyder, C. W., and Matthews, M. S., University of Arizona Press, pp. 835-933.

Biographical Sketch for PI Paul Withers

Center for Space Physics
Boston University
725 Commonwealth Avenue
Boston MA 02215

Tel: (617) 353 1531
Fax: (617) 353 6463
Email: withers@bu.edu
Citizenship: British

Education

- PhD, Planetary Science, University of Arizona 2003
- MS, Physics, Cambridge University, Great Britain 1998
- BA, Physics, Cambridge University, Great Britain 1998

Recent Professional Experience

- Research associate Dr. Michael Mendillo (Boston Univ) 2003-present
Analysis of ionospheric data from Mars and Earth, plus numerical modelling
- Graduate research assistant Dr. Stephen Bougher (Univ. of Arizona) 1998 – 2003
Studied weather in the martian upper atmosphere. Played an advisory role in mission operations for Mars Global Surveyor and Mars Odyssey aerobraking

Fellowships, Honors, and Awards

- CEDAR Postdoctoral Fellowship from NSF for upper atmospheric research 2003
- Kuiper Memorial Award from the University of Arizona for excellence 2002
in academic work and research in planetary science.

Selected Peer Reviewed Publications and Other Major Publications

- Crosby, Bothmer, Facius, Griessmeier, Moussas, Panasyuk, Romanova, and **Withers** “Interplanetary Space Weather and its Planetary Connection” (2007) *Space Weather*, under review.
- Christou, Vaubaillon, and **Withers** “The dust trail complex of comet 79P/du Toit-Hartley and meteor outbursts at Mars” (2007) *Astronomy and Astrophysics*, in press.
- **Withers** “A technique to determine the mean molecular mass of a planetary atmosphere using pressure and temperature measurements made by an entry probe: Demonstration using Huygens data” (2007) *Planetary and Space Science*, 55, in press, 10.1016/j.pss.2007.04.009.
- Montabone, Lewis, Read, and **Withers** “Reconstructing the weather on Mars at the time of the MERs and Beagle 2 landings” (2006) *Geophysical Research Letters*, 33, L19202, doi:10.1029/2006GL026565.
- **Withers** and Smith “Atmospheric entry profiles from the Mars Exploration Rovers Spirit and Opportunity” (2006) *Icarus*, 185, 133-142, doi:10.1016/j.icarus.2006.06.013.
- Mendillo, **Withers**, Hinson, Rishbeth, and Reinisch “Effects of solar flares on the ionosphere of Mars” (2006) *Science*, 311, 1135-1138.

- Bougher and 4 colleagues, including **Withers** “Polar warming in in the Mars thermosphere: Seasonal variations owing to changing insolation and dust distributions” (2006) *Geophysical Research Letters*, 33, L02203, doi:10.1029/2005GL024059.
- **Withers** “Mars Global Surveyor and Mars Odyssey Accelerometer observations of the martian upper atmosphere during aerobraking” (2006) *Geophysical Research Letters*, 33, L02201, doi:10.1029/2005GL024447.
- Fulchignoni and 42 colleagues, including **Withers** “In situ measurements of the physical characteristics of Titan's environment” (2005), *Nature*, **438**, 785-791, doi:10.1038/nature04314.
- **Withers** and Mendillo “Response of peak electron densities in the martian ionosphere to day-to-day changes in solar flux due to solar rotation” (2005) *Planetary and Space Science*, **53**, 1401-1418, doi:10.1016/j.pss.2005.07.010.
- **Withers** “What is a planet?” (2005) *Eos*, **86**(36), 326, doi:10.1029/2005EO360004.
- **Withers**, Mendillo, Rishbeth, Hinson, and Arkani-Hamed “Ionospheric characteristics above Martian crustal magnetic anomalies” (2005) *Geophysical Research Letters*, **32**, L16204, doi:10.1029/2005GL023483.
- **Withers**, Bougher, and Keating, “The Effects of Topographically-Controlled Thermal Tides in the Martian Upper Atmosphere as seen by the MGS Accelerometer”, (2003) *Icarus*, **164**, 14-32.
- **Withers**, Towner, Hathi, and Zarnecki, “Analysis of entry accelerometer data: A case study of Mars Pathfinder”, (2003) *Planetary and Space Science*, **51**, 541-561.
- **Withers** and Neumann, “Enigmatic northern plains of Mars” (2001) *Nature*, **410**, 651.
- **Withers**, “Meteor storm evidence against the recent formation of lunar crater Giordano Bruno” (2001) *Meteoritics and Planetary Science*, **36**, 525 – 529.

Professional Activities and Service

- Reviewer of MER, MRO, Huygens, and Rosetta for NASA PDS and ESA 2004 - present
- Review panel member for NASA Mars Data Analysis Program, NASA Planetary Atmospheres Program, NASA Venus Express Participating Scientist Program, NASA Mars Fundamental Research program, NSF Astronomy and Astrophysics Research Grants Program 2004 - present
- Reviewer for Advances in Space Research, Annales Geophysicae, Icarus, Journal of Geophysical Research, Journal of Spacecraft and Rockets, Mars, Meteoritics and Planetary Science, Planetary and Space Science, and Science. 2001 - present
- Funded co-investigator on NASA Mars Scout Phase A grant for “The Great Escape” mission 2007
- Huygens SSP and HASI/ACC Team Member 2005 - present
- NASA 2003 Mars Exploration Rovers – Atmospheric Advisory Team. 2002 – 2004
- Beagle 2 Environmental Sensor Suite Team Member 2001 - 2003

Professional Affiliations: Member of the American Geophysical Union’s Planetary Sciences Section, the American Astronomical Society’s Division for Planetary Science, and the British Planetary Forum.

Biographical Sketch for Co-I Jean-Loup Bertaux

Service d'Aéronomie du C.N.R.S.
(Centre National de la Recherche Scientifique)
BP 3, 91371 VERRIERES LE BUISSON
France

Tel: +33 1 6920 3116
Fax: +33 1 6920 2999
Email: bertaux@aerov.jussieu.fr

PhD, Geophysics, University of Paris, France, 1974

Recent Professional Experience

2007 - present Senior Research Associate, Boston University
2007 - present Emeritus Director of Research, Service d'Aéronomie, France
2000 - 2007 Director of Research, Service d'Aéronomie, France

PI for SWAN instrument on SOHO, SPICAM instrument on Mars Express, SPICAV instrument on Venus Express. Also had major responsibilities for GOMOS instrument on ENVISAT-1

Selected Publications

- Bertaux, J.-L., and Clarke, J. C. (1989) Deuterium content of the Venus atmosphere, *Nature*, 338, 567-568.
- Bertaux, J.-L., and Montmessin, F. (2001) Isotopic fractionation through water vapor condensation: The deuteropause, a cold trap for deuterium in the atmosphere of Mars, *J. Geophys. Res.*, 106, 32879-32884.
- Bertaux, J.-L. and 27 colleagues (2004) SPICAM: Studying the global structure and composition of the martian atmosphere, *ESA Special Publication 1240*, 95-120, available online at sci.esa.int/science-e/www/object/doc.cfm?fobjectid=34882
- Bertaux, J.-L. and 10 colleagues (2005) Nightglow in the upper atmosphere of Mars and implications for atmospheric transport, *Science*, 307, 566-569.
- Bertaux, J.-L., Leblanc, F., Witasse, O., Quemérais, E., Lilenstein, J., Stern, S. A., Sandel, B., and Korablev, O. (2005) Discovery of an aurora on Mars, *Nature*, 435, 790-794.
- Bertaux, J.-L. and 15 colleagues (2006) SPICAM on Mars Express: Observing modes and overview of UV spectrometer data and scientific results, *J. Geophys. Res.*, 111, E10S90, doi:10.1029/2006JE002690.

Biographical Sketch for Co-I John Clarke

Present Position: Professor
Dept. of Astronomy and Center for Space Physics
Boston University
725 Commonwealth Ave
Boston MA 02115
(617)-353-0247 email: jclarke@bu.edu

Education: Ph.D (Physics) the Johns Hopkins University 1980
M.A. (Physics) the Johns Hopkins University 1978
B.S. (Physics) Denison University 1974

Previous Positions: 1987 - 2001: Research Scientist, University of Michigan

1985-1987: Advanced Instruments Scientist, Hubble Space Telescope Project, NASA Goddard Space Flight Center

1984-1985: Associate Project Scientist, Hubble Space Telescope Project, NASA Marshall Space Flight Center

1980-1984: Assistant Research Physicist, Space Sciences Laboratory, University of California, Berkeley

Selected Refereed Publications:

1. "Identification of the UV Nightglow from Venus", P.D. Feldman, H.W. Moos, J.T. Clarke, and A.L. Lane, *Nature*, 279, 221 (1979).
2. "Detection of Auroral H Ly α Emission from Uranus", J.T. Clarke, *Astrophys. J. Lett.*, 263, L105 (1982).
3. "A Search for the Deuterium Lyman-alpha Emission from the Atmosphere of Mars", J.-L. Bertaux, J.T. Clarke, M. Mumma, T. Owen, and E. Quemerais, *Science with the Hubble Space Telescope*, ESO Proc. No. 44, 459 (1993).
4. "Ultraviolet Remote Sensing Techniques for Planetary Aeronomy", J.T. Clarke and L. Paxton, chapter in "Atmospheres in the Solar System: Comparative Aeronomy", AGU Monograph 130, p. 339 (2002).
5. "Jupiter's Aurora", J.T. Clarke, D. Grodent, S. Cowley, E. Bunce, J. Connerney, and T. Satoh, in *Jupiter*, ed. F. Bagenal et al., Cambridge University Press, ISBN 0-521-81808-7, 2004, p. 639 - 670 (2004).
6. "Morphological Differences Between Saturn's Ultraviolet Aurorae and those of Earth and Jupiter", J.T. Clarke, and 12 co-authors, *Nature*, 433, 717-719 (2005).